II.F.2 Solar High-Temperature Water-Splitting Cycle with Quantum Boost

Ali T-Raissi (Primary Contact), Nazim Muradov, Cunping Huang, Suzanne Fenton, David L. Block, Pyoungho Choi, Jong Baik, Vincent Storhaug, Robin Taylor[1], Roger Davenport[1], David Genders[2], Peter Symons[2]

Florida Solar Energy Center (FSEC)
1679 Clearlake Road
Cocoa, FL 32922
Phone: (321) 638-1446; Fax: (321) 504-3438
E-mail: ali@fsec.ucf.edu
[1]Science Applications International, Corp. (SAIC)
[2]Electrosynthesis Co., Inc.

DOE Technology Development Manager: Rick Farmer
Phone: (202) 586-1623; Fax: (202) 586-2373
E-mail: Richard.Farmer@ee.doe.gov

DOE Project Officer: Lea Yancey
Phone: (303) 275-4944; Fax: (303) 275-4753
E-mail: Lea.Yancey@go.doe.gov

Contract Number: DE-FG36-07GO17002

Subcontractors:
- University of Central Florida, Florida Solar Energy Center, Cocoa, FL
- Electrosynthesis Co., Inc., Lancaster, NY

Project Start Date: September 1, 2007
Project End Date: August 31, 2011

Objectives

- Conduct technoeconomic analysis of photo/thermo-chemical water splitting cycles that can employ, advantageously, solar resource for the production of hydrogen.
- Select a cycle that has the best potential for cost-effective production of hydrogen from water and meeting the 2017 DOE target of $3.00/gge at the plant gate ($4.00/gge delivered).
- Demonstrate technical feasibility of the selected cycle in bench-scale.
- Show pre-commercial feasibility through economic analysis of the selected cycle and demonstration of a fully-integrated pilot-scale solar hydrogen production system.
- Perform techno-economic analysis of the selected cycle having a production capacity of 100 metric ton of hydrogen per day.

Technical Barriers

This project addresses the following technical barriers from the Production section (3.1.4) of the Hydrogen, Fuel Cells and Infrastructure Technologies Program Multi-Year Research, Development and Demonstration Plan:

(U) High-Temperature Thermochemical Technology

(V) High-Temperature Robust Materials

(W) Concentrated Solar Energy Capital Cost

(X) Coupling Concentrated Solar Energy and Thermochemical Cycles

Technical Targets

Table 1 presents the progress made, to date, in achieving the DOE technical targets as outlined in the §3.1.4 Multi-Year Research, Development and Demonstration Plan – Planned Program Activities for 2005-2017 (updated Oct. 2007 version), Table 3.1.9: Solar-Driven, Thermo-chemical High-Temperature Thermochemical Hydrogen Production.

TABLE 1. Progress towards Meeting Technical Targets for Solar-Driven High-Temperature Thermochemical Hydrogen Production

Characteristics	Units	U.S. DOE Targets			Project Status
		2008	2012	2017	
Solar-Driven High-Temperature TCWSC Hydrogen Production Cost	$/gge H_2	10.00	6.00	3.00	5.73[a]
Heliostat Capital Cost (installed cost)	$/m^2	180	140	80	105
Process Energy Efficiency[b]	%	25	30	>35	25.82[c]

[a] Based on revised TIAX reviewed H2A analysis of the photocatalytic sulfur-ammonia (SA) cycle (with dedicated photoreactor field).
[b] Plant energy efficiency is defined as the energy of the hydrogen produced (lower heating value) divided by the sum of the energy delivered by the solar concentrator system plus any other net energy required for the process.
[c] Electrolytic SA cycle efficiency is based on the most recent Aspen flow sheet analysis – see "Economic Analysis" section of the report.
TCWSC - thermochemical water splitting cycle; gge – gasoline gallon equivalent

Accomplishments

- Completed evaluation of the photocatalytic SA hydrogen production cycle and determined that the cycle enjoys high efficiency. However, further improvements in the technology and substantial component cost reductions are needed in order for the photocatalytic SA cycle to achieve the DOE long-term production cost target of $3.00/kg of hydrogen.

- Initiated work on a new modification to the SA cycle that replaced photocatalytic process with an electrolytic one to conduct ammonium sulfite oxidation reaction.
- Identified an alternative sub-cycle to zinc sulfate/ZnO sub-cycle for oxygen production that is based on the all-liquid $K_2SO_4/K_2S_2O_7$ chemistry. Began study of associated reactions. This all-liquid sub-cycle will have a maximum temperature of less than 550°C if the relatively minor power required for the SO_3 decomposition to SO_2 is provided by on-site generated power.
- Fabricated a half-scale prototype glass-reinforced concrete (GRC) heliostat to demonstrate fabrication and design features for a full-scale system.
- Refined the Aspen™ flowsheet of the SA cycle with the $K_2SO_4/K_2S_2O_7$ replacing $ZnSO_4/ZnO$ sub-cycle for oxygen production and an electrolytic process replacing the photocatalytic step for hydrogen generation.
- Determined hydrogen production costs of $5.31/kg for the photocatalytic SA cycle with $ZnSO_4/ZnO$ sub-cycle.

Introduction

A limitation of most solar thermochemical cycles proposed for water splitting is that they do not take advantage of the unique characteristics of the solar resource. For example, the spectrum of sun light contains ultraviolet and visible photons that are very energetic and able to trigger photocatalytic reactions. Most solar thermochemical cycles ignore the potential of these photons and use their energy only as heat to drive thermochemical reactions. In the photocatalytic SA cycle, the photonic portion of solar spectrum is used directly to accomplish the hydrogen evolution step of the cycle. This means that less exergy is needed in the high-temperature oxygen production part of the cycle leading to comparatively lower operating temperatures and reduced requirements on the heliostat field and its associated costs.

Many thermochemical water splitting cycles, studied to date, have difficult and/or costly product separation steps, and materials handling and safety challenges. An example of the former is the Zn/ZnO cycle that requires rapid quenching of the high-temperature Zn-O_2 mixture to prevent unwanted back-reaction to ZnO. An example of later is the Cd/CdO cycle that involves handling and processing of toxic cadmium metal at high temperatures. On the other hand, the sulfur-ammonia cycle has potential to circumvent these and other shortcomings of the legacy thermochemical water splitting cycles while meeting the DOE hydrogen production cost targets.

Approach

To achieve the project objectives, the Bowman-Westinghouse "sulfur-family", hybrid thermochemical water splitting cycle ("Hybrid Sulfur, HyS" cycle) was selected and modified by introducing ammonia as working reagent (thus sulfur-ammonia, SA, cycle) to attain more efficient solar interface and less problematic chemical separation steps. Several versions of the SA cycle were developed and evaluated – experimentally as well as analytically (using AspenPlus™ chemical process simulator).

Two approaches were considered for the hydrogen production step of the SA cycle, namely: photocatalytic and electrolytic oxidation of ammonium sulfite to ammonium sulfate in an aqueous solution. Also, two sub-cycles were evaluated for the oxygen evolution side of the SA cycle, namely: zinc sulfate/zinc oxide and potassium sulfate/potassium pyrosulfate sub-cycles. The laboratory testing and optimization of all the process steps for each version of the SA cycle were then carried out. Once the optimum configuration of the SA cycle has been identified and cycle validated in closed loop operation in the lab, it will be scaled up and on-sun tested.

Results

Cycle Evaluation and Analysis

The first version of the SA cycle employed a photocatalytic reaction step for generating hydrogen and a zinc sulfate/zinc oxide sub-cycle for oxygen generation. The SA cycle also provided an option to split the solar spectrum so that shorter wavelength photons could be diverted to the photocatalytic reactors while lower-energy, longer-wavelength solar heat (>520 nm) redirected to power and drive the oxygen production reactions. Reactions involved in the photocatalytic SA cycle are given below:

$$SO_{2(g)} + 2NH_{3(g)} + H_2O_{(l)} \rightarrow (NH_4)_2SO_{3(aq)} \quad \text{(1 - chemical absorption)} \quad 25°C$$

$$(NH_4)_2SO_{3(aq)} + H_2O_{(l)} \rightarrow (NH_4)_2SO_{4(aq)} + H_2 \quad \text{(2 - solar photocatalytic)} \quad 80°C$$

$$(NH_4)_2SO_{4(s)} + ZnO_{(s)} \rightarrow 2NH_{3(g)} + ZnSO_{4(s)} + H_2O \quad \text{(3 - solar thermocatalytic)} \quad 500°C$$

$$ZnSO_{4(s)} \rightarrow SO_{2(g)} + ZnO_{(s)} + \tfrac{1}{2}O_2 \quad \text{(4 - solar thermocatalytic)} \quad 950°C$$

The photocatalytic step (2) occurs at near ambient temperatures under one sun irradiation. Therefore, photoreactors can be inexpensive and made from low-cost materials. The oxygen production step (4) provides facile separation of O_2 from SO_2 and water vapor. Reactions (3) and (4) form a sub-cycle by which ZnO is reacted with ammonium sulfate, in the low temperature reactor, to form zinc sulfate that is fed to the high

temperature reactor wherein it is decomposed to SO_2, O_2 and ZnO. Zinc oxide is returned to the low-temperature reactor – closing the sub-cycle. The net cycle reaction (represented by reactions 1-4) is decomposition of water to form hydrogen and oxygen. All of the reaction steps described above have been demonstrated in the laboratory and shown to occur without undesirable side reactions.

In the course of Fiscal Year 2008 activities, it was shown that the most active co-catalysts for conducting the hydrogen production step were noble metals (*e.g.* Pt, Pd, Ru, Rh, Ag, and Au) and transition-metal oxides like NiO promote H_2 evolution. Among noble metal promoters, Pt is the most efficient and often used for photocatalytic H_2 production. We have prepared a novel and highly efficient CdS-supported Pd-Cr_2O_3 nano-composite co-catalyst. To determine the relative activity of Pd-Cr_2O_3/CdS in relation to Pt/CdS, CdS was doped with 0.5 wt% of Pt (Pt/CdS) and its photocatalytic activity was measured under the same experimental conditions as those employed for evaluating Pd-Cr_2O_3/CdS. Figure 1 depicts results obtained for the hydrogen evolution rate of Pd-Cr_2O_3/CdS photocatalyst and that of Pt/CdS. The data reveal that doping CdS with Pd-Cr_2O_3 co-catalyst is as effective as and a less expensive alternative to Pt doping of CdS for photocatalytic production of hydrogen from ammonium sulfite.

Based on the Aspen™ chemical process simulation of the photocatalytic-SA cycle, splitting the solar spectrum leads to reasonably high solar-to-hydrogen energy conversion efficiencies. However, these optical losses mean a larger heliostat field is needed in order to conduct heat driven higher temperature oxygen production sub-cycle. Moreover, the present cost of the dichroic mirrors needed for beam splitting is quite high. Both these aspects lead to higher hydrogen production costs. On the other hand, if a dual field configuration is used so that the photocatalytic and thermolytic processes utilize physically separate heliostat fields, the overall costs are lower, but the solar-to-hydrogen energy conversion efficiency will be low.

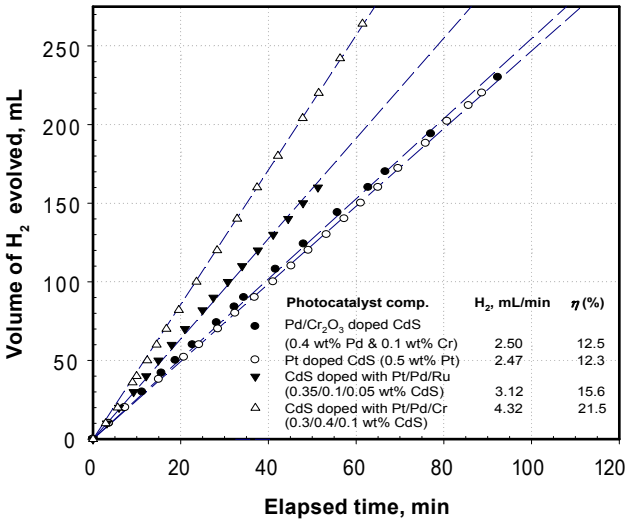

FIGURE 1. Hydrogen evolution vs. time for metal doped cadmium sulfide (CdS) photocatalysts – CdS loading: 1.67 g/L of 1.0 M $(NH_4)_2SO_3$; size of photoreactor window (A_W) = 122.7 cm^2; irradiance ($\Delta\lambda$ = 300-500 nm) $I_{\Delta\lambda}$ = 294.4 W/m^2; η = (H_2 evolution rate x lower heating value of H_2)/(A_W x $I_{\Delta\lambda}$).

At the October 2008 Solar Thermochemical Hydrogen (STCH) Production team meeting held at the DOE Golden Field Office and the January 2009 Technical Team Review meeting at University of Nevada, Las Vegas that followed, we were instructed to consider electro-oxidation, rather than photocatalytic oxidation, of aqueous ammonium sulfite solutions as the hydrogen production step of the SA cycle. The rationale for this was that substituting an electrolytic step for the photocatalytic step may produce a hydrogen production process that is more efficient, has lower overall cost, and higher likelihood of meeting U.S. DOE cost and efficiency targets for solar thermochemical hydrogen production (see Table 1).

In order to accelerate development of a viable electrolytic process for oxidation of aqueous ammonium sulfite to ammonium sulfate, we added a new team member experienced and highly skilled electrochemical company – Electrosynthesis Company (ESC), Inc. Figure 2 depicts a simple mass and energy flow diagram of the proposed electrolytic SA cycle.

Electro-Oxidation of Aqueous Ammonium Sulfite Solutions

Parallel experiments were conducted at FSEC and ESC to determine the optimum process conditions for the electro-oxidation of aqueous ammonium sulfite to ammonium sulfate and hydrogen. Experiments conducted at ESC employed a membrane electrode assembly (MEA) composed of a cast NRE212 membrane coated on one side with fine platinum particles at Pt loading of about 100 μg/cm^2. In an effort to minimize the anode overpotential, the gap between current collector and membrane was reduced to about 1 mm with about 3 mm of felt in the flow space. The flow frames were filled with felt to support the current collectors and provide sufficient contact between the current collectors and active components. The active surface area of the ESC cell was 10 cm^2. Anolyte was 250 mL of 2 M $(NH_4)_2SO_3$ (pH of 8.3) and catholyte consisted of 250 mL of deionized water adjusted to a pH of 9.8 using NH_4OH.

Figure 3 depicts the current-voltage (I-V) curve obtained for the ESC cell at 80°C. The cell voltage for this experiment was about 200 mV lower than an

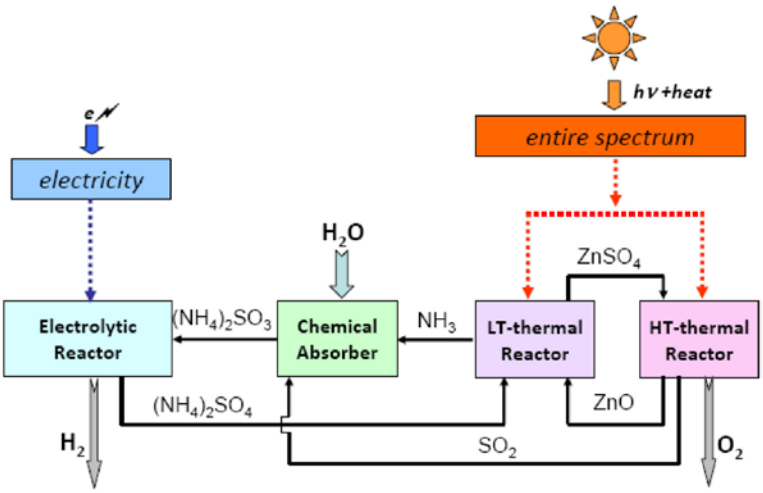

FIGURE 2. Schematic Representation of the Electrolytic SA Cycle

identical cell with anode side MEA platinum loading of 2 μg/cm^2 implying that higher Pt loading is beneficial to reducing cell potential. The rate of H_2 production for this test was 23.0 ± 0.1 mL/min indicating a cell current efficiency of 100% – note that the theoretical H_2 production rate at 3 A cell current is 22.8 mL/min.

At the high current density and high temperatures, the cathode reaction was quantitative with respect to hydrogen formation. However, when run occurred at low current density that resulted in a lower hydrogen production efficiency. The data obtained at the ESC seem to imply that for higher performance, it is more advantageous to operate the cell at high temperatures in order to lower the cell potential.

The decomposition of ammonium sulfite to ammonia, SO_2 and water at high cell operating temperatures does not represent a loss in efficiency (this occurs regardless of whether the electrode is polarized or not) and can be recovered by scrubbing the decomposition gases into ammonium bisulfite solution at room temperature and recovered and returned to the anolyte.

Ammonia is stripped from ammonium hydroxide at higher temperatures but this can be suppressed by elevating the cell operating pressure. Ammonia can also be scrubbed back into the anolyte to prevent its pH from dropping excessively (see Figure 3). Keeping the ammonia concentration low has the added benefit of decreasing the overpotential on the cathode.

Furthermore, the flow sheet analysis of the electrolytic SA cycle has shown that the energy needed to operate the electrolysis plant can be generated on-site using waste heat to produce steam. The electrolytic system can operate 24/7 and requires a much smaller footprint than does the photocatalytic process.

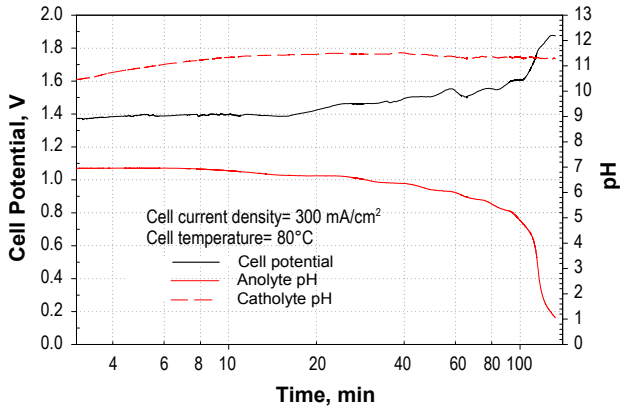

FIGURE 3. Variation of cell voltage, anolyte pH and catholyte pH vs. time for the ESC test cell V (graphite felt divider anode, GFD3, provided by SGL-Carbon Group, NRE212 membrane, MEA cathode with ~100 μg Pt/cm^2, grooved graphite current collectors) operating at 80°C and fixed current density of 300 mA/cm^2.

Another issue that came up at the October 2008 STCH team meeting held at DOE Golden Field Office related to design of the high temperature reactors that make up the SA cycle's O_2 production sub-cycle and solids handling and transport from one reactor to the other. In order to address this concern, we modified the processes involved in the oxygen production sub-cycle of the SA cycle and replaced them with all liquid processes described in the following.

Aspen™ Flow Sheet of the Electrolytic SA Cycle with $K_2SO_4/K_2S_2O_7$ Sub-Cycle

The high-temperature reactions of the electrolytic SA cycle can be modified to allow an all fluid materials transport instead of having to handle solid reagents. The new chemistry replaces earlier reactions (3) and (4) with the following reactions:

$$(NH_4)_2SO_{4(aq)} + K_2SO_{4(l)} \rightarrow K_2S_2O_{7(l)} + 2NH_{3(g)} + H_2O_{(g)}$$ (5 – solar thermal) 400°C

$$K_2S_2O_{7(l)} \rightarrow K_2SO_{4(l)} + SO_{3(g)}$$ (6 – solar thermal) 550°C

$$SO_{3(g)} \rightarrow SO_{2(g)} + \tfrac{1}{2}\, O_{2(g)}$$ (7 – solar thermal) 850°C

The advantages of the new sub-cycle are, among others:

Simplified material handling – The liquid $K_2SO_4/K_2S_2O_7$ mixture can be pumped through pipes rather than bucket lifting and/or conveyor transport needed for the earlier $ZnO/ZnSO_4$ sub-cycle.

Lower temperature step – Reaction (5) is carried out at 400°C which is readily available by employing parabolic trough solar concentrating technology. This can result in more efficient and cost-effective operation as compared to the power tower approach.

Simplified thermal storage and energy recovery – Storage of and energy recovery from the liquid $K_2SO_4/K_2S_2O_7$ system can be achieved via existing technology and does not require complex and elaborate engineering and construction.

The most recent Aspen™ flow sheet of the electrolytic SA cycle with all liquid $K_2SO_4/K_2S_2O_7$ sub-cycle developed at FSEC is shown in Figure 4. Hydrogen is produced at a rate of 5,556 kg/hr based on 24 hr/day operation in the ELECTROL electrolysis reactor according to reaction (2). The reactor is operated at 2 bar pressure. Theoretical power input to the electrolyzer is 96 MW (based on an experimental cell running at 94°C, 0.65 V cell potential and current density of 70.4 mA/cm^2 with 100% current efficiency). The hydrogen gas is separated from steam in a flash unit FL-H2 and compressed to produce 5,556 kg/hr H_2 with molar purity of 98% at 21.7 bar.

The aqueous ammonium sulfate solution produced in ELECTROL passes through a series of heat exchangers for preheating prior to entering the solar thermal reactor LOTEMRXN which performs reaction (5). Hot product gases from this reactor (NH_3 and H_2O) are easily separated from molten salt $K_2S_2O_7$ and expanded in a turbine (TURBINE1) to produce electricity. These gases are condensed in TOWER 2 (simulating a condensing turbine), mixed with recycled and makeup water, and fed to SFIT-GEN reactor where reaction (1) occurs. The molten $K_2S_2O_7$ exiting the LOTEMRXN is converted to gaseous and liquid products via reaction (6) that is carried out at 550°C (represented in the Aspen™ flow sheet by a second reactor MIDTEMRX).

The product SO_3 gas from reaction (6) is preheated in HX-5 and fed to a third solar thermal reactor (represented by HITEMRXN), where reaction (7) is performed at 850-1000°C. The gaseous products from reaction (7) are used to preheat the incoming SO_3, compressed and fed to SFIT-GEN reactor. SO_2/O_2 and NH_3/H_2O streams are reacted exothermically according to reaction (1) to produce aqueous ammonium sulfite $(NH_4)_2SO_3$ solution and a gaseous H_2O/O_2 stream in SFIT-GEN. The solution generated by reaction (1) is fed back to the electrolytic reactor. The gaseous products are cooled and condensed via cooling tower (TOWER). Oxygen is released from the system (represented by flash FL-O2). Cooled water exiting FL-O2 is combined with NH_3/H_2O stream exiting TOWER2. The resulting stream is pumped into SFIT-GEN.

We note that: reaction (5) in LOTEMRXN reactor can be carried out in a parabolic trough type solar receiver/reactor. Reaction (6) in MIDTEMRX reactor

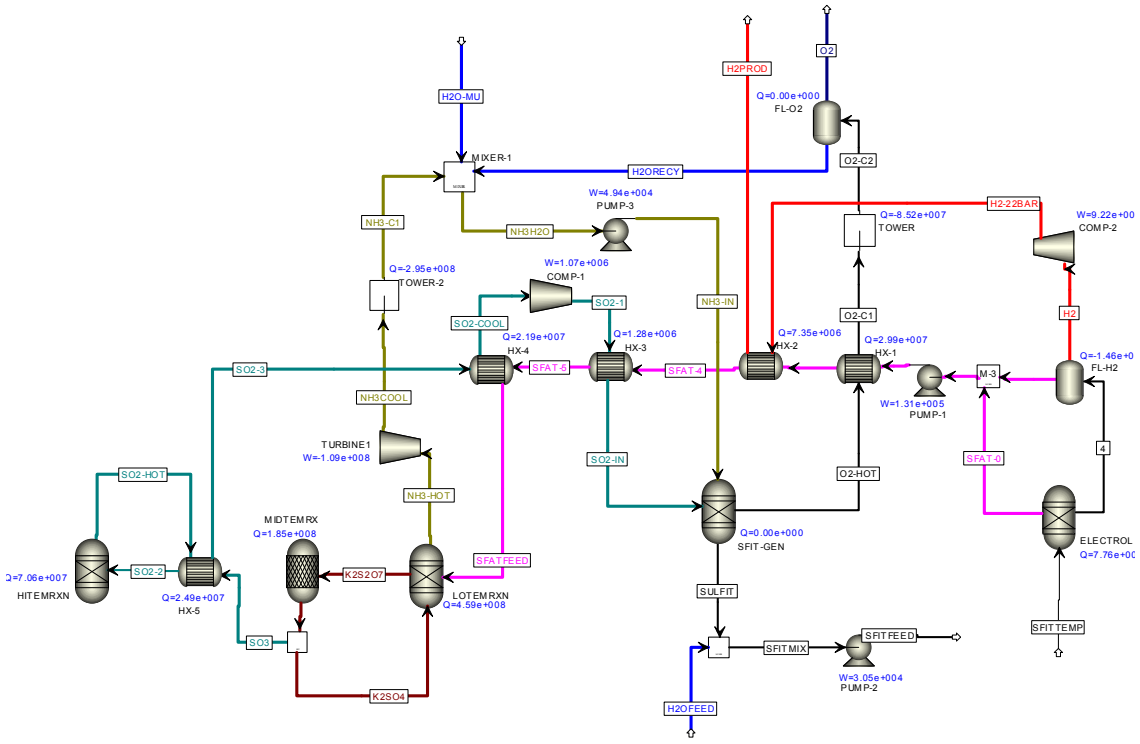

FIGURE 4. AspenPlus™ Flow Sheet for the Electrolytic SA Cycle with $K_2SO_4/K_2S_2O_7$ Sub-Cycle

can be performed in a series of tubes running through a power tower receiver. Reaction (7) that occurs in HITEMRXN reactor can be carried out in a bayonet type solar reactor operated in a power tower receiver. The ELECTROL reaction is still under development at ESC and FSEC. The SFIT-GEN reaction occurs spontaneously and evolves heat.

In this analysis, we used a ratio of 8 moles of H_2O per mole of $(NH_4)_2SO_3$. Lower ratios can be tolerated if the stream temperatures and pressures are adjusted to prevent precipitation of salt. The electrolyzer power requirement of 96.015 MW estimated from the laboratory data (for a two-dimensional cell operating at 94°C, Nafion® 211 membrane coated with 0.4 mg/cm^2 Pt and graphite current collectors) is close to the theoretical value calculated using Faraday's law with the cell potential of 0.65 V and hydrogen molar flow rate of 2,756 kmol/hr (for 24 hr around the clock electrolyzer operation). This is due to the fact that the cell current efficiency was essentially 100%.

The calculated efficiency of the electrolytic SA cycle (with $K_2SO_4/K_2S_2O_7$ sub-cycle) from the flow sheet depicted in Figure 4 was 18.7% (lower heating value). This calculation took account of the energy produced by TURBINE1 minus the energy needed to operate the electrolysis plant, compressors and pumps.

Solar Concentrator Configuration for Photocatalytic SA System

Several configurations were evaluated for the photocatalytic SA system. Beam-splitting systems were found to be more expensive due to the cost of beam-splitting mirrors and because the heliostat field needs to be 30-40% larger if beam splitting is used. The best configuration for a beam-splitting system was found to be a North-field heliostat field with full-spectrum mirrors, a "cold" mirror at the top of the tower that redirects the ultraviolet/visible light back down to the ground level, and a photoreactor field located south of the tower that receives about two suns worth of ultraviolet/visible (one from the sun and one from the reflected light from the cold mirror). This design maximized the solar efficiency of the photocatalytic SA system.

The most cost-effective photocatalytic SA system design was determined to be a system with a heliostat/power tower feeding energy to the high-temperature reactors, and a separate flat-plate photoreactor field. This was less "efficient" due to the land usage for the large flat-plate photoreactor field, but the cost was less due to having a smaller heliostat field and not needing beam-splitting mirrors.

Solar Field Optimization

In this year, the design of a heliostat field was further refined and evaluated. A computer model was built using hour-by-hour TMY3 weather data for Barstow, CA to generate annual performance estimates for the heliostat field. Using H2A and Sargent & Lundy cost data the capital cost for the heliostat field was developed and used to optimize the heliostat field for minimum energy cost. The optimum field was found to have a 90 m tower with about 68,000 m^2 of heliostats over a land area of 49 acres.

A conceptual design of a receiver configuration suitable for the SA cycle was developed. Approximately 1/3 of the thermal energy is needed at the highest temperature of approximately 800-850ºC. Based on a square heliostat size of 10 m^2, and using the actual sun size, an estimate of the potential concentration and image size from heliostats within the field was developed. For the high temperature reactor a rectangular aperture of 6 m by 6m was chosen to minimize the amount of optical spillage at the receiver. Similarly, for the lower temperature reactor, at 350ºC, an aperture of 8.5 m by 8.5 m was selected. The reason for the larger aperture at the lower temperature is that the energy for that receiver would be delivered from the heliostats furthest from the tower, where beam spread is the greatest.

The solar field configuration is continuing to be updated as the thermochemical system evolves. The primary present activity is to incorporate the all-liquid $K_2SO_4/K_2S_2O_7$ system.

Heliostat Cost Reduction

The design of a GRC-based heliostat system has continued. A preliminary design was developed, and a half-scale prototype GRC heliostat has been fabricated and is being tested (see Figure 5). The purpose of the prototype was to develop and demonstrate fabrication techniques and design features for the full-scale system.

The design features a factory-cast heliostat structure with reinforcements and mounting provisions built-in, and a factory-cast foundation ring with integral azimuth drive features. The elevation drive is actuated with a linear actuator of the type used for satellite dishes. The azimuth drive uses a "spring-worm" drive design developed by SAIC several years ago, with the loops of a coil spring acting as the teeth of a ring gear. A prototype control system was developed using a microprocessor-based controller with solar photovoltaic power and wireless communication. Evaluation of the prototype will be completed, and a final design of a full-scale unit will be finished so that a production cost analysis can be completed.

FIGURE 5. SAIC GRC Heliostat Design

Economic Analysis

The photocatalytic SA process with separate heliostat and photoreactor fields was analyzed using the H2A economic model. The resulting cost for hydrogen was found to be $5.73. The cost analysis of the electrolytic SA cycle is underway. The preliminary cost figures for the electrolysis plant have been determined. Tables 2 and 3 provide the basis for calculating the cell and module capital costs, respectively. The data in these tables have been estimated from recently published information for the HyS thermochemical hydrogen production cycle [1].

TABLE 2. Basis for Cell Capital Costs

Item	Description	Cost Basis	$/m^2
Membrane	NRE212 or equiv	$300/m^2	300
Gas diffusion layers	Porous carbon	$75/m^2 (2 layers)	150
Electrocatalyst	0.3 mg/cm^2 Pt (total)	$1,500/troy oz	150
Bipolar plates	3/8" graphite	$200/m^2	200
Seals, gaskets, etc.	PEEK or equivalent	$50/m^2	50
Cell assembly	Automated	1 man-hr at $50/man-hr	50
Single cell cost			900

PEEK – Polyether ether ether ketone

Each module has been assumed to contain 230 cells (each incorporating a 1 m^2 of active area) to which the following cost items have been added:

Installed costs were calculated for the electrolysis plant of the SA cycle using cost assumptions of the Tables 2 and 3 for cell fabrication and applying TIAX

TABLE 3. Module Capital Costs

Item	Description	Cost Basis	$/m^2
Cells	230 units	$900/m^2 (see **Table 2**)	900
End plates, tie rods, and other pressure comp.	Carbon steel	$23,000	100
Current collectors and connection to direct current bus	Copper	$9,200	40
Assembly	Off site	64 man-hr at $50/man-hr	20
Overhead	Manufacturing	20% of materials and labor	192
Module Cost			1,252
Balance of Electrolyzer System (BOES) Contribution			648
Total Including BOES Contribution			**1,900**

installation factor of 1.2. The installed capital cost of the electrolytic plant of the SA cycle calculated based on the best laboratory test data obtained to date (for which the total required membrane area is approximately 209,800 m^2) is estimated to be about $204.4 per metric ton of hydrogen produced. Note that the electrolytic SA cycle generates 109 MW of power that is more than that needed to run the electrolysis plant (*i.e.*, 96.015 MW). Total on-site power consumption including that required for the compressors and pumps, is about 106.5 MW. Total power input into the high temperature SO_3 decomposition reactor is about 70.6 MW which is considerably less than that generated on-site.

Conclusions and Future Directions

In summary:

- The photocatalytic SA cycle has been shown to be technically feasible and able to achieve high efficiency. However, further improvements in the technology and substantial components cost reduction are necessary in order for the photocatalytic SA cycle to achieve the DOE cost target of $3.00/kg of hydrogen produced by 2017.
- The electrolytic SA cycle is in early development stage, so further performance improvements and cost reductions are likely.
- Based on the work performed to date, it appears that the electrolytic SA cycle has potential to meet DOE's near- and long-term H_2 production cost and efficiency goals.
- GRC has promise to reduce heliostat cost substantially.

Activities planned for the upcoming year include:

- Completion of phase 1 activities.
- Documentation of the photocatalytic SA cycle results.
- Finalization of the thermal reactor/receiver design.
- Conclusion of the solar field configuration and design.

With respect to the electrolysis work, we note that both the anodic oxidation of sulfite and cathodic H_2 evolution reaction are pH dependent,

$$SO_4^{2-} + 4\ H^+ + 2\ e^- \rightarrow H_2SO_3 + H_2O$$

$$E^0 = +0.172\ \text{V/normal hydrogen electrode}$$

$$SO_4^{2-} + H_2O + 2\ e^- \rightarrow SO_3^{2-} + 2OH^-$$

$$E^0 = 0.930\ \text{V/normal hydrogen electrode}$$

The main source of voltage loss is due to the anode losses. Therefore, future activities in this area will be focused on reducing the cell voltage by finding conditions that allow anode function at high pH without adverse effect on localized pH changes. One approach is to introduce some buffering capacity into the solution.

Future plans include additional work to:

- Identify catalysts that will reduce the over-potential at the anode and allow operation at high current densities.
- Complete the electrolytic hydrogen production and electrolytic cell optimization tests.
- Finalize the electrolytic SA cycle H2A analysis.

We should also note that there is some disagreement involving measurement of the rate of electrolytic hydrogen production performed at FSEC and ESC evidenced by differences in current density obtained by the cells at the respected laboratories. Efforts are underway to resolve measurement issues by testing and verifying ESC cell performance independently at FSEC.

Future activities involving the solar interface include:

- Recombine anolyte and catholyte streams to control and maintain fixed pH.
- Refine solar field and receiver design as the chemical plant needs evolve.
- Conduct detailed production cost estimate for GRC heliostat system based on prototype test results.
- Complete the design of a full-scale prototype of pre-commercial GRC heliostat design.

Finally, assuming a "GO" decision by the U.S. DOE, the next phase of the project will involve laboratory demonstration and validation of the closed-loop SA cycle followed by on-sun hydrogen production demonstration.

Special Recognitions & Awards/Patents Issued

1. Huang, C., T-Raissi, A., Muradov, N.Z. "Solar Metal Sulfate – Ammonia Based Thermo-chemical Water Splitting Cycles for Hydrogen Production," Utility Patent Application No. 12/267,569, Nov., 8, **2008**.

2. Huang, C., Yao, W., Muradov, N.Z., T-Raissi, A. "Non-Pt Based Pd-Cr_2O_3/CdS Photocatalysts for Solar Photocatalytic Hydrogen Production," Provisional Patent filed March **2009**.

FY 2009 Publications/Presentations

1. Yao, W., Huang, C., Muradov, N.Z., T-Raissi, A. "Photocatalytic H_2 Evolution on Visible Light Illuminated CdS Supported Pd-Cr_2O_3 Nanocomposite Cocatalyst Using Regenerable Sacrificial Donor," Paper submitted to the *J. of the American Chemical Society*.

2. Taylor, R. T-Raissi, A. Davenport, R. "Solar Hydrogen Production Through High-Efficiency Thermochemical Water Splitting with Photocatalytic or Electrolytic Steps," *SOLAR 2009* (ASES National Solar Conference), Buffalo, NY, 11–16 May **2009**.

3. Taylor, R., Davenport, R., T-Raissi, A., Muradov N., Huang C., Fenton S., Block D. "Solar Hydrogen Production Through Thermochemical Water Splitting with Photocatalytic or Electrolytic Steps," *National Hydrogen Association Conf. & Expo*, Columbia, South Carolina, April **2009**.

4. T-Raissi, A., Fenton, S. "H2A Analysis of the Photocatalytic Sulfur-Ammonia Cycle – Revised Analysis," delivered to TIAX, March **2009**.

5. T-Raissi, A., Taylor, R., Davenport, R. Presentation at the *STCH Meeting*, University of Nevada at Las Vegas, January 22, **2009**.

6. Taylor, R., T-Raissi, A., Davenport, R. Presentation at the *STCH Meeting*, DOE Golden Field Office, October 8–9, **2008**.

References

1. Gorensek, M.B., Summers, W.A., Bolthrunis, C.O., Lahoda, E.J., Allen, D.T., Greyvenstein, R. "Hybrid Sulfur Process Reference Design and Cost Analysis," Final Report, U.S. DOE Contract No. DE-AC09-08SR22470, SRNL-L1200-2008-00002, REV 1, 12 June **2009**.